



## Short communication

# Second derivative techniques in differential scanning calorimetry of DNA modified with platinum compounds



Chun-Ling Chang<sup>a</sup>, Chun-Chung Chen<sup>a</sup>, Chin-Kun Hu<sup>a,b,c,\*</sup>, Dmitri Y. Lando<sup>a,d,\*</sup>

<sup>a</sup> Institute of Physics, Academia Sinica, Nankang, Taipei 11529, Taiwan

<sup>b</sup> National Center for Theoretical Sciences, National Tsing Hua University, Hsinchu 30013, Taiwan

<sup>c</sup> Business School, University of Shanghai for Science and Technology, Shanghai 200093, China

<sup>d</sup> Institute of Bioorganic Chemistry, National Academy of Sciences of Belarus, 220141, Minsk, Belarus

## ARTICLE INFO

## Keywords:

DNA complexes with platinum compounds  
DNA differential scanning calorimetry  
Second derivative techniques in calorimetry  
Complex DNA systems

## ABSTRACT

The second derivative techniques, which are used in spectroscopy to reveal poorly resolved bands, were adjusted for processing of calorimetric melting profiles of DNAs from higher organisms. The procedure strongly increased the sensitivity of the profiles to various distortions of the double helix and allowed clear resolution of the constituents arising from the melting of satellite DNA (minor narrow peaks) and the rest of genome (dominant wide peak). As an illustration of the advantages of the procedure, selective suppression of narrow satellite peaks was demonstrated as DNA was chemically modified by the antitumor drug cisplatin. As the cisplatin/nucleotide molar ratio increased from 0.001 to 0.05, the peaks decreased in height until they fully disappeared. The influence of cisplatin on the shape of the main peak, which corresponds to the rest of the genome, was much weaker. Transplatin, an ineffective analog of cisplatin, suppressed all constituents of the melting profile without selectivity.

## 1. Introduction

Second derivative techniques are used in spectroscopy and differential scanning calorimetry (DSC) of polymers and biopolymers to reveal poorly resolved peaks [1]. In a negative second derivative curve, peak maxima coincide with the positions of the initial peaks, but the initial widths are decreased [2] which improves resolution. Another property is selective suppression of wide peaks and emphasis of narrow ones [2]. In this study, the method was adjusted for processing of calorimetric melting profiles of DNAs of higher organisms and applied to DNA chemically modified with platinum compounds. The procedure strongly increased the sensitivity of DNA calorimetric melting profiles to various distortions of the double helix and allowed clear resolution of their two constituents arising from melting of satellite DNA and the rest of genome.

Platinum antitumor compounds exert their anticancer activity by chemical modification of DNA. Satellite DNA is the main component of centromeres that are essential in cell division. Since normal cell division is altered by cancer [3], the second derivative techniques was applied to calorimetric profiles of DNA chemically modified with the antitumor platinum drug cisplatin to reveal the thermodynamic peculiarities of the cisplatin's influence on satellite DNA.

Calorimetric melting profiles of DNA of higher organisms, include two very dissimilar overlapped parts [4–9]. The minor part corresponding to satellite DNA with quasi-periodical sequences is represented by narrow peaks (#1–4 in Fig. 1A, gray line). Those peaks stand out against a wide main peak (#0 in Fig. 1A, red line) originated from melting of the rest of the genome. DNAs from ten different higher organisms we have studied display very similar shapes of their main wide peak (see also [8,9]). At the same time, the number, height, temperature position and relative area of narrow satellite peaks vary among different DNAs. For the ten DNAs we have investigated, the peaks of satellite DNA are most clearly seen in DSC melting profile of Calf Thymus DNA. Therefore, Calf Thymus DNA is the most suitable for the thermodynamic investigation of the influence of platination on satellite DNA.

However, for the differential scanning calorimeter CSC 6300 NanoDSC and Calf Thymus DNA used in our study, a traditional way of differentiation [10] is impossible. Numerical calculation of the second derivative introduce artifacts into the results due to noise in the data. The common procedure used to suppress noise distorts the shape of the second derivative curve. Here we propose two ways to overcome that problem and illustrate the use of one of the ways to resolve the constituents arising from melting of satellite DNA and the rest of genome.

\* Corresponding authors at: Institute of Bioorganic Chemistry, National Academy of Sciences of Belarus, 220141, Minsk, Belarus; Institute of Physics, Academia Sinica, Nankang, Taipei 11529, Taiwan.

E-mail addresses: [clchang1024@gate.sinica.edu.tw](mailto:clchang1024@gate.sinica.edu.tw) (C.-L. Chang), [cjj@phys.sinica.edu.tw](mailto:cjj@phys.sinica.edu.tw) (C.-C. Chen), [huck@phys.sinica.edu.tw](mailto:huck@phys.sinica.edu.tw) (C.-K. Hu), [dmitrilando@gmail.com](mailto:dmitrilando@gmail.com) (D.Y. Lando).

<http://dx.doi.org/10.1016/j.tca.2017.05.022>

Received 10 October 2016; Received in revised form 30 April 2017; Accepted 30 May 2017

Available online 03 June 2017

0040-6031/ © 2017 Elsevier B.V. All rights reserved.

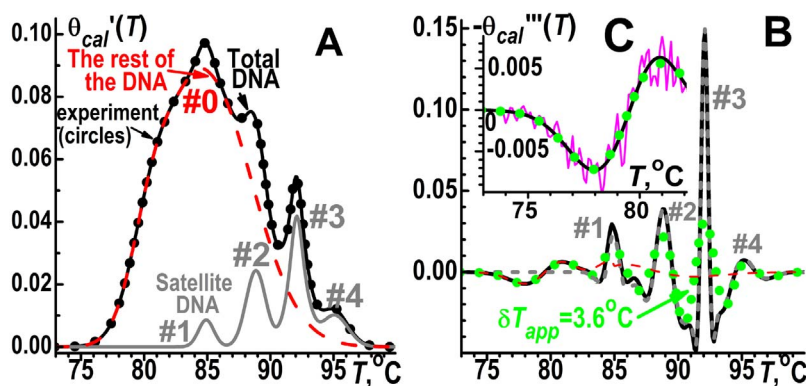


Fig. 1. (A) The experimental calorimetric differential melting curve (cDMC) of unmodified Calf Thymus DNA [ $\theta_{cal}'(T)$ , black circles], the results of its deconvolution with Gaussian functions into four narrow peaks (#1–#4, satellite DNA, gray) and wide main peak (#0, the rest of the genome, red). The simulated cDMC (the sum of Gaussian functions) is shown with black solid line. (B, C) Negative second derivatives [ $-\theta_{cal}''(T)$ ] calculated analytically for the simulated cDMC (black) and for its constituents (red and gray) shown in Fig. 1A. Green circles (B,C) represent coinciding results of the numerical differentiation at  $\delta T_{app} = 3.6$  °C of both experimental and simulated calorimetric cDMCs. The “jagged” line in Fig. 1C shows strong noise in second derivative calculated for experimental cDMC at  $\delta T_{app} = 0.4$  °C. (For interpretation of the references to colour in this figure legend, the reader is referred to the web version of this article.)

The procedure also clearly demonstrates how the constituents are altered under platination.

## 2. Materials and methods

For platination, Calf Thymus DNA was incubated in 10 mM NaClO<sub>4</sub> during 48 h at 37 °C in the dark at pH ~ 6 with cisplatin or transplatin produced by Sigma-Aldrich Corporation. The Pt/nucleotide molar ratio  $r$  was 0.001–0.05. It is known that, after such incubation, cisplatin reacts with DNA quantitatively ( $r_b = r$ ) forming mainly bifunctional products if  $r \leq 0.1$  [11–13].

Raw calorimetric melting profiles were obtained with differential scanning calorimeter CSC 6300 NanoDSC (Calorimetry Sciences Corporation, USA) at [NaCl] = 110 mM, 5 mM cacodylic acid, 0.1 mM EDTA, pH 7, DNA concentration 1 mg/mL, heating rate 1 °C/min.

Since the temperature intervals between points were not uniform (on the average ~0.017 °C), the raw data and buffer (instrumental) baseline were recalculated for a given uniform step  $h = 0.02$ –0.1 °C by linear interpolation between two nearest points of raw data. The helix-coil transition excess heat capacity  $C_p$  (Fig. 2A and D) was obtained by subtraction of the buffer baseline from raw data, correction for difference in heat capacity of DNA before and after melting (subtraction of transition baseline), and normalization to molar concentration of base pairs [14–17]. Calorimetric differential melting curve [cDMC,  $\theta_{cal}'(T)$ ] (black circles in Fig. 1A) was calculated as the transition excess heat capacity  $C_p(T)$  normalized to area under the curve  $C_p(T)$  (to the enthalpy  $\Delta H$ ) [14–17]:

$$\theta_{cal}'(T) = C_p(T) / \int_{T_s}^{T_e} C_p(T) \cdot dT = C_p(T) / \Delta H \quad (1)$$

where  $T_s$  and  $T_e$  are the temperatures of the start and end of the helix-coil transition, respectively;  $\Delta H$  is the calorimetric enthalpy of the helix-coil transition. In the DSC experiments, we followed standard procedures [14]. The calorimetric melting curve  $\theta_{cal}(T)$  is the integrated form of  $\theta_{cal}'(T)$ , i.e.,  $\theta_{cal}(T)$  is the temperature dependence of the fraction of the heat absorbed under the helix-coil transition [16,17]. It is the analog of the DNA melting curve that is the temperature dependence of the fraction of melted base pairs. Thus, the second derivative of normalized melting profile  $\theta_{cal}'(T)$  (cDMC) is the third derivative  $\theta_{cal}''(T)$  of the calorimetric melting curve  $\theta_{cal}(T)$ .

## 3. Results

### 3.1. Numerical and analytical differentiation of experimental and simulated cDMCs

To smooth noise and calculate the negative second derivative [ $-\theta_{cal}''(T)$ ] of the calorimetric differential melting curve  $\theta_{cal}'(T)$ , we primarily used the standard Savitzky-Golay method [10]. Each point of the function  $\theta_{cal}'(T)$  was considered as the center of the interval of

$p = 2m + 1$  neighboring points that are approximated by a polynomial of degree  $n$ . Using the polynomial coefficients, the derivative(s) was calculated for the central,  $(m + 1)$ -th, point.

The first derivative [ $\theta_{cal}'(T)$ ] was primarily calculated for the calorimetric cDMC  $\theta_{cal}'(T)$ . Then approximation and differentiation procedures were repeated in the same way for  $\theta_{cal}(T)$  to obtain the second derivative [ $\theta_{cal}''(T)$ ] of the cDMC  $\theta_{cal}'(T)$ . Such an approach gives much smaller distortions of  $\theta_{cal}'(T)$  than direct computation of the second derivative from the first polynomial approximation. In this study, the polynomial degree was  $n = 3$ .

For suppression of higher noise level at a given value of the step  $h$ , a larger number of neighboring points  $p$  is necessary in each approximation. More exactly, a larger temperature region of approximation around each point,  $\delta T_{app} = (p-1)h$ , is necessary to calculate second derivative of  $\theta_{cal}'(T)$ . For the DNA calorimetric profiles obtained with CSC 6300 NanoDSC, we found the following peculiarities:

- (1) The results of differentiation were mainly determined by the  $\delta T_{app}$  value and almost independent of the  $h$  value if  $h \leq 0.1$  °C.
- (2) A value of  $\delta T_{app} \geq 1.4$  °C was required for valid noise suppression, i.e., the value  $\delta T_{app} = 1.4$  °C was the minimal that gives coincidence of the second derivatives of 5 experimental curves that were different if  $\delta T_{app} < 1.4$  °C because of non-reproducible undepressed noise. The noise is clearly seen in Fig. 1C for one of those curves obtained at  $\delta T_{app} = 0.4$  °C (pink “jagged” line).

For evaluation of distortions caused by numerical double differentiation, we used the results of analytical calculations. Experimental calorimetric cDMC of Calf Thymus DNA (black circles in Fig. 1A) was deconvoluted with Gaussian functions into four narrow peaks #1–#4 corresponding to satellite DNA (gray line) and main wide asymmetric peak #0 corresponding to the rest of the DNA (red line). The simulated cDMC calculated as the sum of all Gaussian constituents #0–#4 (black solid line) is close to experiment. The average relative deviation is ~0.3%. Simulated cDMC allows the exact analytical calculation of undistorted second derivatives for further determination of distortions caused by numerical differentiation. Numerical double differentiation of the simulated cDMC at various  $\delta T_{app}$  values and comparison of those results with the exact analytical calculation allows the choice of maximal  $\delta T_{app}$  that does not distort the second derivative.

The two constituents and their sum (simulated cDMC) shown in Fig. 1A were doubly differentiated analytically (Fig. 1B, black line) and numerically for values of  $\delta T_{app} = 0.4$  °C–3.7 °C. Comparison of analytical (“exact”) and numerical (“approximate”) calculation of the second derivative of the simulated cDMC curve demonstrated that distortions in the shape caused by numerical differentiation procedure became acceptable at  $\delta T_{app} \leq 0.4$  °C for all melting interval (75 °C <  $T$  < 98 °C) (Fig. 1B). However, as was mentioned above, valid noise suppression in DNA calorimetric profiles occurs at much larger  $\delta T_{app}$  values ( $\geq 1.4$  °C). Calculations demonstrate that the maximums of narrow

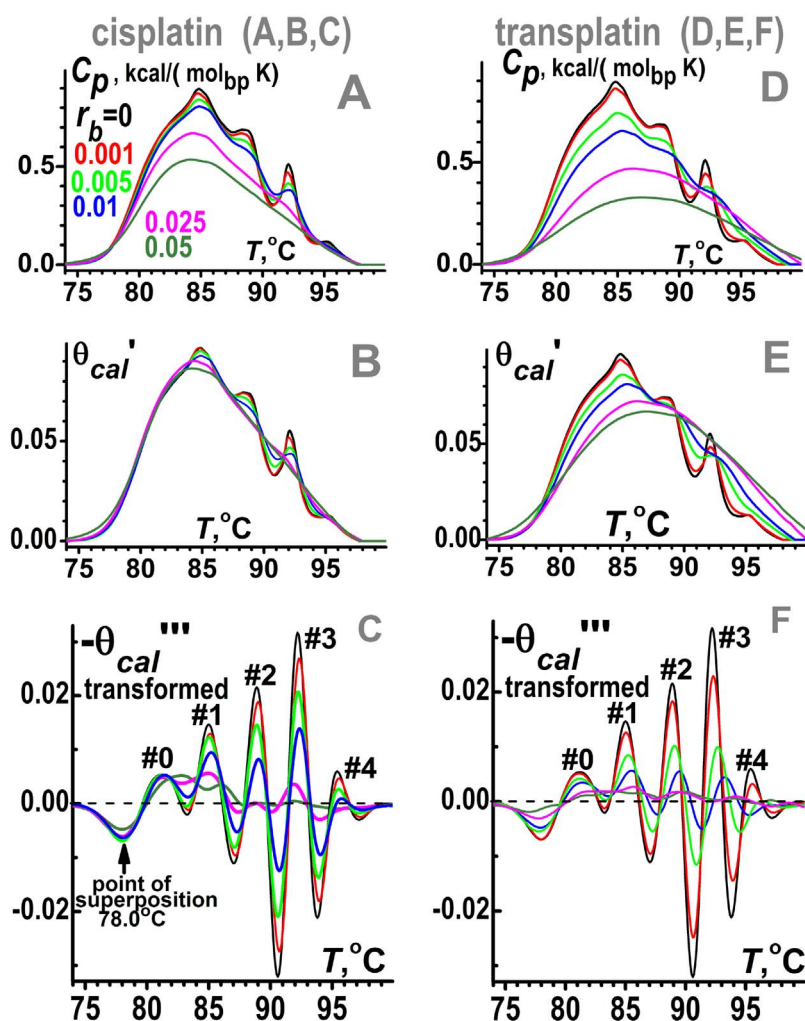


Fig. 2. The transition excess heat capacity  $C_p$  (A,D), calorimetric cDMC  $\theta_{cal}'$  (B,E) and its transformed negative second derivative  $-\theta_{cal}'''(T)$  (C,F) for various Pt/nucleotide molar ratios  $r_b$ . All curves corresponding to DNA modification with cisplatin (A,B,C,  $r_b = 0.001$ –0.05) were shifted to make the positions of their low temperature minimum in (C) the same as for unmodified DNA ( $r_b = 0$ , = 78.0 °C, shown with arrow). For  $r_b = 0.05$ , the shift is maximal and equal to +5.2 °C. There is no shift for transplatin (D,E,F,  $r_b = 0.001$ –0.05).

peaks in the second derivative curves are underestimated at  $\delta T_{app} = 1.4$  °C. The height of the highest peak #3 in negative second derivative of the simulated cDMC is 1.5 times smaller relative to analytical differentiation and/or numerical differentiation at  $\delta T_{app} = 0.4$  °C. It demonstrates that, for the differential scanning calorimeter CSC 6300 NanoDSC and Calf Thymus DNA, the traditional direct way of differentiation [10] is impossible because of too strong noise.

At the same time, negative second derivative calculated analytically for the simulated curve (black line) coincides with numerical calculations in the temperature region without satellite peaks (75 °C <  $T$  < 83 °C) for  $\delta T_{app} \leq 3.6$  °C (Fig. 1C). In that temperature region, second derivative of experimental cDMC calculated for  $\delta T_{app} = 1.4$  °C–3.6 °C demonstrate full noise suppression and coincidence with analytical derivative of the simulated cDMC (green circles correspond to  $\delta T_{app} = 3.6$  °C).

Thus, numerical differentiation of the experimental calorimetric cDMC at  $\delta T_{app} = 0.4$  °C demonstrates strong noise in the region without satellite peaks 75 °C <  $T$  < 83 °C (Fig. 1C, pink “jagged” line). However, the average absolute value of the negative second derivative  $[-\theta_{cal}'''(T)]$  is 20–40 times higher in the temperature region of narrow peaks (83 °C <  $T$  < 98 °C, Fig. 1B). Therefore, relative noise value is low even for  $\delta T_{app} \leq 0.4$  °C.

Those results suggest the use of two different values of  $\delta T_{app}$  for calculation in different temperature regions. The value  $\delta T_{app} = 3.6$  °C can be used for differentiation in the region which does not include satellite peaks (75 °C <  $T$  < 83 °C). For the region of satellite peaks (83 °C <  $T$  < 98 °C), the value of  $\delta T_{app} \leq 0.4$  °C should be employed

in the calculation. This procedure does not fully suppress noise over the whole calorimetric profile, but it strongly decreases the noise/signal ratio with minor shape distortion of second derivative.

Statistical confirmation of the approach that includes the two  $\delta T_{app}$  values for different temperature regions follows from a comparison of the average values of cDMC and of the noise. The average of absolute value of noise shown with pink “jagged” line in Fig. 1C was calculated as the average sum of the absolute values of the differences between second derivatives of experimental calorimetric cDMC calculated at  $\delta T_{app} = 0.4$  °C and at  $\delta T_{app} = 3.6$  °C in the temperature region without satellite peaks (75 °C <  $T$  < 83 °C). This average noise value for second derivatives is equal to  $(1.31$ – $1.42) \cdot 10^{-3}$ . The average value of the second derivatives in this temperature region is  $(3.80$ – $3.85) \cdot 10^{-3}$ . Thus, the average relative noise value is ~30% for the considered region. However, the average value of second derivatives of the simulated  $\theta_{cal}'(T_i)$  in the region of satellite peaks (83 °C <  $T$  < 98 °C) is much higher  $[(21.4$ – $21.5) \cdot 10^{-3}$  (Fig. 1B)]. The noise absolute value and structure are approximately the same for all DNA melting interval. Therefore, the relative noise value account for 6% at 83 °C <  $T$  < 98 °C. This is an acceptable value for the use of the second derivative techniques.

In the curves of “real” second derivatives calculated with the use of two  $\delta T_{app}$  values [ $3.6$  °C at 75 °C <  $T$  < 83 °C and  $0.4$  °C at 83 °C <  $T$  < 98 °C], there is a strong decrease in heights of narrow peaks under platinumation especially at low  $r_b$ . For cisplatin, the height of peak #3 decreases by 32% at  $r_b = 0.001$ ; 71% at  $r_b = 0.005$  and about 95% at  $r_b = 0.025$  (not shown). For transplatin, the nonuniformity is even stronger: 50%, 84%, and 100%, respectively (not shown).

The use of this algorithm for platinated DNAs will be expanded elsewhere.

### 3.2. Transformed negative second derivative of cDMC ( $\delta T_{app} = 3.6^\circ\text{C}$ )

As follows from Fig. 1B, the negative second derivative techniques provides an opportunity to reveal narrow peaks for studies of different factors on satellite DNA. The main peak corresponding to the rest genome is also seen at temperatures where satellite peaks are absent ( $75^\circ\text{C} < T < 83^\circ\text{C}$ , Fig. 1B and C). However, the relative height of the main peak is too small to determine the influence of various factors on the rest of the genome.

If numerical differentiation of entire cDMC is carried out with  $\delta T_{app} = 3.6^\circ\text{C}$ , the heights of narrow peaks are decreased relative to the real values and become comparable with the height of the main peak corresponding to the rest of the genome. The second derivative of the main peak does not change height and shape at  $\delta T_{app} = 3.6^\circ\text{C}$  relative to analytical differentiation (Fig. 1B and C, circles).

Using differentiation at  $\delta T_{app} = 3.6^\circ\text{C}$ , one can simultaneously follow the change of all peaks under various distortions of DNA structure. At the same time, the noise is validly suppressed in whole cDMC at  $\delta T_{app} = 3.6^\circ\text{C}$ . The proposed approach is suitable at much higher level of noise typical for calorimeters produced earlier than the calorimeter CSC 6300 NanoDSC used in our present study.

Thus, the use of  $\delta T_{app} = 3.6^\circ\text{C}$  transforms the negative second derivative and makes it more suitable to study DNA platination. For the transformed negative second derivative ( $\delta T_{app} = 3.6^\circ\text{C}$  for all DNA melting interval  $75^\circ\text{C} < T < 98^\circ\text{C}$ ), a change in heights of narrow peaks with the degree of platination  $r_b$  becomes much more monotonic than for the “real second derivative”. However, the high sensitivity of satellite peaks to platination is conserved in the transformed second derivative curves. A change is clearly recognizable at  $r_b = 0.001$  for both cisplatin ( $14.2\% \pm 1.9\%$ ) and transplatin ( $28.5\% \pm 2.6\%$ ) (Fig. 2C and F).

## 4. Discussion

As observed in Fig. 1A, narrow peaks of satellite DNA are not well resolved in the cDMC of total DNA  $\Theta_{cal}'(T)$ . In contrast, the satellite peaks prevail in the curve of the negative second derivative  $[-\Theta_{cal}''(T)]$  and determine its shape in the temperature region  $83^\circ\text{C} < T < 98^\circ\text{C}$  (Fig. 1B).

As the Pt/nucleotide molar ratio  $r_b$  increases from 0.001 to 0.05 the curve of the transition excess heat capacity  $C_p$  decreases its height (Fig. 2A and D). This indicates the general decrease in the enthalpy of the helix-coil transition caused by cisplatin and transplatin. Cisplatin reduces DNA melting temperature, and transplatin slightly raises it (see also [5]). Besides general decrease in the  $C_p$ , a change in the shape of the curves is also seen. To observe the changes more clearly the  $C_p$  curves were normalized to the areas (to the enthalpies, Eq. (1)). Such normalization gives calorimetric differential melting curve [cDMC,  $\Theta_{cal}'(T)$ ] (Fig. 2B and E). The calorimetric cDMCs demonstrate that narrow peaks of satellite DNA selectively decrease under platination (see also [4,5]) and become unresolved without second derivative technique. The details of their elimination are not seen against the background of the wide main peak, which is shown separately in Fig. 1A and B (red).

Second derivative techniques demonstrate that cisplatin selectively suppresses narrow peaks corresponding to satellite DNA without a change in their shape (Fig. 2C and F). As the cisplatin/nucleotide molar ratio increased from 0.001 to 0.05, the peaks #1–#4 originating from melting of satellite DNA decreased in height right up to their full disappearance. In contrast, there is no change in height of the main peak (#0) corresponding to the rest of the genome at  $r_b = 0.001$ –0.025. Transplatin, cisplatin's ineffective analog, demonstrates stronger suppression of satellite peaks but smaller selectivity (Fig. 2C and F). It

decreases the heights of all peaks (#0–#4). Sonication of DNA solution also unselectively influences the shape of both parts of cDMC similar to transplatin (not shown).

As other examples of the use of second derivative techniques, we have assessed the degree of DNA distortions caused by conditions used before melting experiments and in melting experiments with platinated DNA. For preparation of DNA complexes with platinum compounds, longtime incubation at  $37^\circ\text{C}$  at low  $\text{Na}^+$  (10 mM  $\text{NaClO}_4$ , pH  $\sim 6$ –7) is often used (see part 2 of this study and works [4,5,11–13]). In melting experiments, alkaline medium (pH = 10.5) is used to increase the impact of platinum compounds on the DNA helix-coil transition [4,7]. Using transformed second derivatives, we have demonstrated that distorting effects in both cases are much smaller than the effect of one platination site per 1000 nucleotides ( $r_b = 0.001$ ).

The transformed negative second derivative is applied in our study because traditional approach [10] cannot be used for calorimetric profiles of DNA of higher organisms registered with the calorimeter CSC 6300 NanoDSC. However, the calorimeter is characterized by a relatively low noise level. For  $\delta T_{app} = 3.6^\circ\text{C}$ , even much stronger noise typical for calorimeters produced earlier is validly suppressed (DASM-4 M, not shown). The approach is also more convenient for comparative studies of unmodified DNAs from various higher organisms. The transformation makes the second derivative curves comparable in value, while real maximal heights can differ 20–40 times as for Bovine (Calf Thymus) DNA and Hen (Chicken) DNA.

## 5. Conclusion

In this study, we propose a new way of applying of second derivative techniques to differential scanning calorimetry and demonstrate that it is an effective tool for investigation of platinated DNAs from higher organisms. The effectiveness is illustrated by separation of the influence of platinum antitumor drug cisplatin and its ineffective analog transplatin on satellite DNA and the rest of the genome.

## Acknowledgements

We are grateful to Prof. R.M. Wartell for helpful comments and editing the text, to Dr. I.E. Grigoryan for registration of DNA melting with calorimeter DASM-4M and for calorimetric study of DNA distortion in alkaline medium. This work was supported by the Ministry of Science and Technology (MOST) of the Republic of China (Taiwan) under Grants MOST 105-2112-M-001-004, MOST 103-2112-M-001-016, MOST 104-2112-M-001 –002 and by National Center for Theoretical Sciences (NCTS) in Taiwan. DYL was supported by Academia Sinica in Taipei. We are grateful to the Biophysics Core Facility, Scientific Instrument Center of Academia Sinica for the use of CSC 6300 NanoDSC differential scanning calorimeter.

## References

- [1] L. Bouzidi, M. Boodhoo, K.L. Humphrey, S.S. Narine, Use of first and second derivatives to accurately determine key parameters of DSC thermographs in lipid crystallization studies, *Thermochim. Acta.* 439 (2005) 94–102.
- [2] H. Mark, J. Workman Jr, *Chemometrics. Derivatives in spectroscopy Part I: the behavior of the derivative*, *Spectroscopy* 18 (4) (2003) 32–37.
- [3] K. Collins, T. Jacks, N.P. Pavletich, The cell cycle and cancer, *Proc. Natl. Acad. Sci. U. S. A.* 94 (1997) 2776–2778.
- [4] D.Y. Lando, E.N. Galyuk, C.-L. Chang, C.-K. Hu, Temporal behavior of DNA thermal stability in the presence of platinum compounds. Role of monofunctional and bifunctional adducts, *J. Inorg. Biochem.* 117 (2012) 164–170.
- [5] D.Y. Lando, C.-L. Chang, A.S. Fridman, I.E. Grigoryan, E.N. Galyuk, Y.-W. Hsueh, C.-K. Hu, Comparative thermal and thermodynamic study of DNA chemically modified with antitumor drug cisplatin and its inactive analog transplatin, *J. Inorg. Biochem.* 137 (2014) 85–93.
- [6] D.Y. Lando, A.S. Fridman, C.-L. Chang, I.E. Grigoryan, E.N. Galyuk, O.N. Murashko, C.-C. Chen, C.-K. Hu, Determination of melting temperature and temperature melting range for DNA with multi-peak differential melting curves, *Analyt. Biochem.* 479 (2015) 28–36.
- [7] E.N. Galyuk, A.S. Fridman, V.I. Vorob'ev, S.G. Haroutunian, S.A. Sargsyan,



- M.M. Hauruk, D.Y. Lando, Compensation of DNA stabilization and destabilization effects caused by cisplatin is partially disturbed in alkaline medium, *J. Biomol. Struct. Dyn.* 25 (2008) 407–418.
- [8] H.H. Klump, Conformational transitions in nucleic acids, in: M.N. Jones (Ed.), *Biochemical Thermodynamics*, 2nd ed., Elsevier, Amsterdam, 1988, pp. 100–143.
- [9] Klump H, Calorimetric studies on DNAs and RNAs, in: W. Saenger (Ed.), *Landolt Börnstein Neue Serie Group VII, vol. 1C*, Biophysik Springer, Berlin, 1990, pp. 241–256.
- [10] A. Savitzky, M.J.E. Golay, Smoothing and differentiation of data by simplified least squares procedures, *Anal. Chem.* 36 (1964) 1627–1639.
- [11] R. Zaludova, V. Kleinwachter, V. Brabec, The effect of ionic strength on melting of DNA modified by platinum(II) complexes, *Biophys. Chem.* 60 (1996) 135–142.
- [12] V. Kleinwachter, H. Rau, A study of DNA interaction with platinum cytostatics, *Stud. Biophys.* 103 (1984) 5–12.
- [13] O. Vrana, V. Brabec, V. Kleinwachter, Polarographic studies on the conformation of some platinum complexes: relations to anti-tumour activity, *Anticancer Drug Des.* 1 (1986) 95–109.
- [14] J. Volker, R.D. Blake, S.G. Delcourt, K.J. Breslauer, High-resolution calorimetric and optical melting profiles of DNA plasmids: resolving contributions from intrinsic melting domains and specifically designed inserts, *Biopolymers* 50 (1999) 303–318.
- [15] E. Freire, Differential scanning calorimetry, *Methods Mol. Biol.* 40 (1995) 191–218.
- [16] C.-L. Chang, A.S. Fridman, I.E. Grigoryan, E.N. Galyuk, O.N. Murashko, C.-K. Hu, D.Y. Lando, Estimation of the diversity between DNA calorimetric profiles, differential melting curves and corresponding melting temperatures, *Biopolymers* 105 (2016) 832–839.
- [17] C.-L. Chang, A.S. Fridman, R.M. Wartell, C.-K. Hu, D.Y. Lando, Relationship between calorimetric profiles and differential melting curves for natural DNAs, *Int. J. Biol. Macromol.* 102 (2017) 591–598.